Chapter 7

Follicle Detection and Ovarian Classification in Digital Ultrasound Images of Ovaries

P. S. Hiremath and Jyothi R. Tegnoor

Additional information is available at the end of the chapter

http://dx.doi.org/10.5772/56518

1. Introduction

Some of the successful applications of the image processing techniques are in the area of medical imaging. The development of sophisticated imaging devices coupled with the advances in algorithms specific to the medical image processing both for diagnostics and therapeutic planning is the key to the wide popularity of the image processing techniques in the field of medical imaging. Ultrasound imaging is one of the methods of obtaining images from inside the human body through the use of high frequency sound waves. The reflected sound wave echoes are recorded and displayed as a real time visual image. It is a useful way of examining many of the body's internal organs including heart, liver, gall bladder, kidneys and ovaries. The detection of follicles in ultrasound images of ovaries is concerned with the follicle monitoring during the diagnostic process of infertility treatment of patients.

For women undergoing assisted reproductive therapy, the ovarian ultrasound imaging has become an effective tool in infertility management. Among the many causes, ovulatory failure or dysfunction is the main cause for infertility. Thus, an ovary is the most frequently ultrasound scanned organ in an infertile woman. Determination of ovarian status and follicle monitoring constitute the first step in the evaluation of an infertile woman. Infertility can also be associated with the growth of a dominant follicle beyond a preovulatory diameter and subsequent formation of a large anovulatory follicle cyst. The ovary is imaged for its morphology (normal, polycystic or multicystic), for its abnormalities (cysta, dermoids, endometriomas, tumors etc), for its follicular growth in ovulation monitoring, for evidence of ovulation and corpus luteum formation and function. Ovulation scans allow the doctor to determine accurately when the egg matures and when it ovulates. Daily scans are done to visualize the growing follicle, which looks like a black bubble on the screen of the ultrasound imaging machine.

1.1. Ovarian types

The outcome of ovarian evaluation is the classification of the ovary into one of the three types of ovaries, namely, normal ovary, cystic ovary and polycystic ovary, which are described below :

i. Normal ovary with antral/dominant follicles

A normal ovary consists of 8-10 follicles from 2mm to 28mm in size [1]. The group of follicles with less than 18mm in size are called antral follicles, and the size in the range of 18-28mm are known as dominant follicles. In a normal menstrual cycle with ovulation, a mature follicle, which is also a cystic structure, develops [2]. The size of a mature follicle that is ready to ovulate is about 18-28mm in diameter. During the past 50 years, it has been accepted that folliculogenesis begins with recruitment of a group or cohort of follicles in the late luteal phase of the preceding menstrual cycle followed by visible follicle growth in the next follicular phase [3]. The group or cohort of follicles begins growth and by the mid-follicular phase, around day 7, a single dominant follicle appears to be selected from the group for accelerated growth [4]. The dominant follicle continues to grow at a rate of about 2mm per day. In women, a preovulatory follicle typically measures 18–28mm when a surge of luteinizing hormone (LH) is released from the pituitary to trigger ovulation; ovulation occurs approximately 36 hours after LH release [5]. The Figure 1 shows an ultrasound image of normal ovary with dominant follicles.

ii. Ovarian cyst

An ovarian cyst is simply a collection of fluid within the normal solid ovary. There are many different types of ovarian cysts, and they are an extremely common gynaecologic problem. Because of the fear of ovarian cancer, cysts are a common cause of concern among women. But, it is important to know that the vast majority of ovarian cysts are not cancer. However, some benign cysts will require treatment, in that they do not go away by themselves, and in quite rare cases, others may be cancerous [6]. The most common types of ovarian cysts are called functional cysts, which result from a collection of fluid forming around a developing egg. Every woman who is ovulating will form a small amount of fluid around the developing egg each month. The combination of the egg, the special fluid-producing cells, and the fluid is called a follicle and is normally about the size of a pea. For unknown reasons, the cells that surround the egg occasionally form too much fluid, and this straw colored fluid expands the ovary from within. If the collection of fluid gets to be larger than a normal follicle, about three-quarters of an inch in diameter, a follicular cyst is said to be present. If fluid continues to be formed, the ovary is stretched as if a balloon was being filled up with water. The covering of the ovary, which is normally white, becomes thin and smooth and appears as a bluish-grey. Rarely, though, follicular cysts may become as large as 3 or 4 inches [7]. The Figure 2 shows an ultrasound image of cystic ovary.

iii. Polycystic ovary

The typical polycystic appearance is defined by the presence of 12 or more follicles measuring less than 9mm in diameter arranged peripherally around a dense core of stroma [8]. Other ultrasound features include enlarged ovaries, increased number of follicles and density of

http://dx.doi.org/10.5772/56518

Figure 1. Ultrasound image of a normal ovary with dominant follicles

ovarian stroma. The current ultrasound guidelines supported by ESHRE/ASRM consensus characterize the polycystic ovary as containing 12 or more follicles measuring 2–9mm [9]. The basic difference between polycystic and normal ovaries is that, although the polycystic ovaries contain many small antral follicles with eggs in them, the follicles do not develop and mature properly, and hence, there is no ovulation [10]. The infertility incidence with polycystic ovaries is very high. These women usually will have difficulty in getting pregnant and, hence, invariably require treatment to improve chances for pregnancy. In a polycystic ovary, the numerous small cystic structures, also called antral follicles, give the ovaries a characteristic "polycystic" (many cysts) appearance in ultrasound image. It is referred to as polycystic ovarian syndrome (PCOS/PCOD) [11]. Since women with polycystic ovaries do not ovulate regularly, they do not get regular menstrual periods. The Figure 3 shows an ultrasound image of ovary with PCOD.

A computer assisted diagnostic procedure is desirable because of tedious and time consuming nature of the manual follicle segmentation and ovarian classification done by medical experts. In the present book chapter, the objective of study is to design algorithms for follicle detection and ovarian classification in ultrasound ovarian images in order to assist medical diagnosis in infertility treatment using digital image processing techniques.

Figure 2. Ultrasound image of a cystic ovary

1.2. Background literature

In [12,13], follicular ultrasound images are segmented using an optimal thresholding method applied to coarsely estimated ovary. However, this fully automated method, using the edges for estimation of ovary boundaries and thresholding as a segmentation method, doesn't give optimal results. In [14], this method has been upgraded using active contours and, consequently, the segmentation quality of recognized follicles is considerably improved. Edges of recognized objects were much closer to the real follicle boundaries. However, the determination of suitable parameters for snakes automatically is problematic. In [15], region growing based segmentation method is used for the follicle detection. In [16], a semi automated method is proposed for the outer follicle wall segmentation, wherein a frequent manual tracing of the inner border of all follicles is done. In [17], cellular automata and cellular neural networks are employed for the follicle segmentation. The results are found to be very promising but an obvious drawback of these two methods is the difficulty in determination of the required parameters for follicle segmentation. In [18], the authors have determined the inner border of all follicles using watershed segmentation techniques. Watershed segmentation was applied on smoothed image data which merged some small adjacent follicles. Therefore binary mathematical morphology was employed to separate such areas adhoc in some steps. In [19],

http://dx.doi.org/10.5772/56518

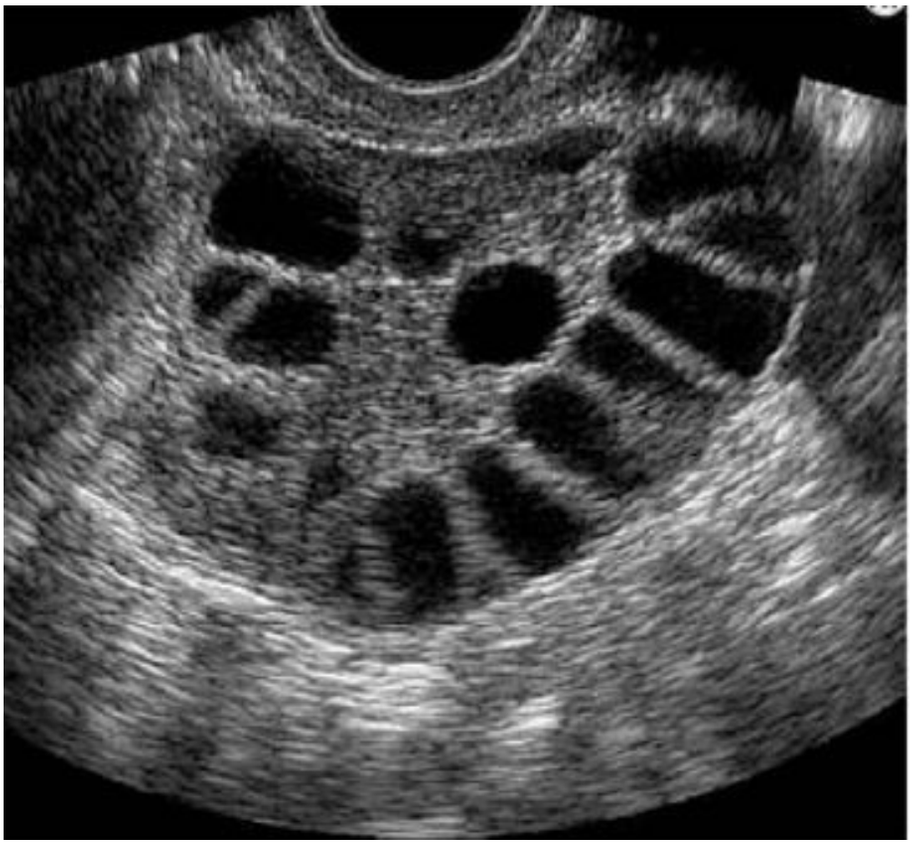

Figure 3. Ultrasound image of an ovary with PCOD

the authors have reported follicle segmentation based on modified region growing method for the follicle segmentation and linear discriminant classifier for the purpose of classification. In [20], the scanline thresholding method is used for the follicle detection and the segmentation performance is measured in terms of the mean square error (MSE).

The follicles are the regions of interest (ROIs) in an ovarian ultrasound image, which need to be detected by using image processing techniques. This is basically an object recognition problem. Thus, the basic image processing steps, namely, preprocessing, segmentation, feature extraction and classification, apply. In the literature, the authors have employed various techniques for ultrasound image processing, as shown below:

1. Preprocessing

- Gaussian low pass filter
- Homogeneous region growing mean filter (HRGMF)
- Contourlet transform

2. Segmentation

- Optimal thresholding
- Edge based method

– Watershed transform

– Scanline thresholding

– Active contour method

3. Feature extraction

– Geometric features

– Texture features

4. Classification

– 3σ interval based classifier.

– K-NN classifier

– Linear discriminant classifier

– Fuzzy classifier

– SVM classifier

1.3. Image data set

For the purpose of experimentation, the databases D1, D2 and D3, of ultrasound images of ovaries are prepared in consultation with the medical expert, namely, Radiologist and Gyneocologist, for the present study of the follicle detection and ovarian classification in ovarian images. Some of the images are captured by the Toshiba [Model SSA-320A/325A] diagnostic ultrasound system with the transvaginal transducer frequency 26 Hz. Some of the images are obtained from the publicly available websites [www.radiologyinfo.com; www.ovaryresearch.com]. The image dataset D1 consists of the 80 ultrasound ovarian images, with the size 256x256. The image dataset D2 consists of the 90 ultrasound ovarian images, with the size 512x512. The image dataset D3 consists of the 70 ultrasound ovarian images, with the size 512x512. It contains the images of 30 normal (healthy) ovaries, 20 polycystic ovaries and 20 cystic ovaries.

2. Follicle detection

The methods employed by [Hiremath and Tegnoor] for follicle detection based on different segmentation, feature extraction and classification techniques are described below:

a. Edge based method

The automatic method for the detection of follicles in ultrasound images of ovaries using edge based method uses, Gaussian lowpass filter for preprocessing, canny operator for edge detection for segmentation, 3σ-intervals around the mean for the purpose of classification [21]. The experimentation has been done using sample ultrasound images of ovaries and the results

http://dx.doi.org/10.5772/56518

are compared with the inferences drawn by medical expert. Initially, the image is processed with Gaussian low pass filter yielding denoised image. Then canny operator is applied to detect the edges from the denoised image. Morphological dilation is performed by using the disk shaped structuring element with radius 1 to fill the weak edges. which yields the segmented image. Possible holes inside the segmented regions are filled. Any spurious regions due to noise are eliminated by morphological erosion. The regions in segmented image having smaller area than the threshold T (empirical value) are removed. The segmented regions are labeled. Set all the nonzero pixels of the border of segmented image to zero, which yields the final segmented image. Thus the plausible follicle regions are the labeled segments.

The geometric features are extracted for the known follicle regions. The main aim of geometric feature extraction is to recognize geometric properties of ovarian follicles in ultrasound images. The ovarian follicles are oval shaped compact structures, which resemble the circular/ellipse and are, thus, characterized by the seven geometric features, namely, the area A, the ratio R of majoraxislength to minoraxislength, the compactness Cp, the circularity Cr, the tortousity Tr, the extent E and the centriod $Y = \frac{1}{B^2}\sum_{i,j=1}^{B} CS_{-i,-j}\left(F^{-1}\left(\lambda\left(F\left(CS_{i,j}(X)\right)\right)\right)\right)$.

The classification stage comprises two steps, namely, the training phase and the testing phase.

Training phase : In the training phase, the geometrical features, are computed for regions known to be follicles in the training images in consultation with the medical expert. Then, the sample means and standard deviations of the geometric parameters R, Cp, Cr, Tr, E and, $C = (Cx, Cy)$ are computed which are used to set the rules for classification of labelled segments into follicles and non-follicles. The $\overline{R}$, $\overline{Cp}$, $\overline{Cr}$, $\overline{Tr}$, $\overline{E}$, $(\overline{Cx}, \overline{Cy})$ denote the mean values, and, the σ_R, σ_{Cp}, σ_{Cr}, σ_{Tr}, σ_E, $(\sigma_{Cx}, \sigma_{Cy})$ denote the standard deviation values, of the geometric parameters R, Cp, Cr, Tr, E and C=(Cx,Cy).

Now, the classification rules for follicle recognition are formulated as following: A region with area A, ratio R, compactness Cp, circularity Cr, Tortousity Tr, extent E, and centriod $C = (Cx, Cy)$, is classified as a follicle, if the following conditions are satisfied:

$$A > T_A \tag{1}$$

$$\overline{R} - \alpha\sigma_R < R < \overline{R} + \alpha\sigma_R \tag{2}$$

$$\overline{Cp} - \alpha\sigma_{Cp} < Cp < \overline{Cp} + \alpha\sigma_{Cp} \tag{3}$$

$$\overline{Cr} - \alpha\sigma_{Cr} < Cr < \overline{Cr} + \alpha\sigma_{Cr} \tag{4}$$

$$\overline{Tr} - \alpha\sigma_{Tr} < Tr < \overline{Tr} + \alpha\sigma_{Tr} \tag{5}$$

$$\overline{E} - \alpha\sigma_{E} < \mathrm{E} < \overline{E} + \alpha\sigma_{E} \tag{6}$$

$$\overline{Cx} - \alpha\sigma_{Cx} < Cx < \overline{Cx} + \alpha\sigma_{Cx} \tag{7}$$

$$\overline{Cy} - \alpha\sigma_{Cy} < Cy < \overline{Cy} + \alpha\sigma_{Cy} \tag{8}$$

The constants T_A and α are empirically determined. In our experiments, we have determined that the empirical values are T_A =30, α=3. The equations (1) to (8) constitute the 3σ-classifier, which is to be used in the testing phase.

Testing phase : During the testing phase, the area A, the ratio R, the compactness Cp, the circularity Cr, the tortousity Tr, the extent E and the centriod, $C=(Cx, Cy)$ are computed for a region of the segmented image and apply the above classification rules to determine whether it is a follicle or not. The comparison of the experimental results for the two sample images with the manual segmentation done by medical expert is presented in the Figure 4. There is good agreement between the segmented image and the manual segmentation done by the medical expert, which demonstrates the efficiency of the edge based method. The manual segmentation is done by the team of three medical experts (Radiologists (2) and Gynaecologist (1)).

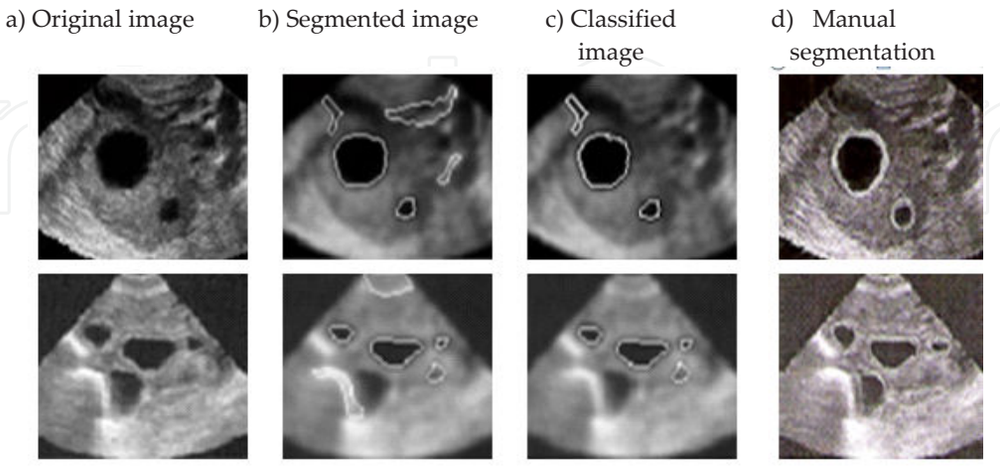

Figure 4. Some typical results: a) Original images, b) Segmentation by edge based method, c) Classified image, d) Manual segmentation by medical expert.

http://dx.doi.org/10.5772/56518

b. Watershed segmentation method

The follicle detection in ultrasound images of ovaries using watershed segmentation method uses the watershed transform for segmentation, geometric features for feature extraction and 3σ-intervals around the mean for the purpose of classification [22]. We follow three steps in the segmentation, first, the internal marker image is obtained, second, external marker image is obtained, and third, modifying gradient of the original image, by mask. In next phase, segmentation is carried out by applying marker controlled watershed transform to modified gradient image, region filling and clearing the border. Finally, preserve the regions which are most probably appear as follicles, while all other regions are removed. The feature extraction is based on seven geometric parameters of the follicles and the classification of regions for follicle detection is based on 3σ intervals around the mean. The experimental results are in good agreement with the manual follicle detection by medical experts.

c. Optimal thresholding method

In the automatic detection of follicle in ultrasound images of ovaries using optimal thresholding method, sobel operator and morphological opening and closing is used for preprocessing, optimal thresholding for segmentation and 3σ-intervals around the mean for classification are used [23]. Initially, the image is processed with finding the gradient by using sobel operators in horizontal direction. For the gradient image morphological opening and closing is applied by using appropriate structuring element. Then thresholding is applied to the filtered image by optimal thresholding method [24]. In the process, many undesired spurious regions are also obtained (e.g., regions inside the endometrium). These spurious regions must be removed as much as possible and all regions touching the borders are removed, which yields the segmented image. The feature extraction is based on seven geometric parameters of the follicles and the classification of regions for follicle detection is based on 3σ intervals around the mean. The experimental results are in good agreement with the manual follicle detection by medical experts.

2.1. HRGMF and thresholding

Ultrasound ovary images show planar sections through the follicles. These images are characterized by specular reflections and edge information, which is weak and discontinuous. Therefore, traditional edge detection techniques (e.g. Sobel, Prewitt) are susceptible to spurious responses when applied to ultrasound imagery. The main reason, that the follicle segmentation using solely edge information is rather unsuccessful, is a high level of added speckle noise [25]. The follicles being fluid-filled sacs appear as dark oval regions because they display similar fluid echotextures, which are more or less darker than their neighbourhood. The follicles could therefore be treated as homogeneous dark regions.

The main idea behind the HRGMF based method is as follows: [26]: In the first phase, the homogeneous region growing mean filter (HRGMF) is applied [27]. By using this filter, first homogeneous region can be identified and then this region is grown until it satisfies the similarity criteria. The value of filtering point is replaced by arithmetic mean of the grown region. In next phase, segmentation is carried out, by binarising the filtered image with three

different thresholds, T1, set as standard deviation of the input image, T2, set as mean of the input image, T3, set as abs(T2-T1). The resultant images are combined after thresholding. The components are labelled, the holes inside the regions are filled, the borders if any are cleared. Finally, the regions which most probably appear as follicles are preserved, while all other regions are removed. The feature extraction is based on seven geometric parameters of the follicles and the classification of regions for follicle detection is based on 3σ intervals around the mean.

The experimentation has been done using two datasets D1 and D2. The D1 set consists of the 80 sample ultrasound ovarian images of size 256x256, out of which 40 images are used for training and 40 for testing. The D2 set consists of 90 sample ultrasound images of ovaries of size 512x512, out of which 45 images are used for training and 45 for testing. The ten-fold experiments are performed for the classification and the average follicle detection rate is computed.The Table 1 shows the classification results of the proposed method after ten-fold experiments for both the data sets D1 and D2. The average detection rates for the proposed method with D1 and D2 sets are 79.77% and 68.86%, false acceptance rates (FAR) are 25.99% and 28.41%, and false rejection rates (FRR) are 20.52% and 31.12%, respectively.

	Classification results for ten-fold experiments	
Data set	D1 set	D2 set
Classification rate	79.77%	68.86%
Type I error (FAR)	25.99%	28.41%
Type II error(FRR)	20.52%	31.12%

Table 1. Classification results of proposed method after ten-fold experiments.

The proposed HRGMF based method for follicle detection is more effective as compared to the edge based method, watershed based segmentation method and optimal thresholding methods. The experimental results are in good agreement with the manual follicle detection by medical experts, and thus demonstrate efficacy of the method. Thus, the proposed HRGMF based method for follicle segmentation is effective in computer assisted fertility diagnosis by the experts.

2.2. Contourlet transform and scanline thresholding

The follicle detection rate in the homogeneous region growing mean filter (HRGMF) based method is considerably improved. However, due to speckle noise, finding the object boundaries is difficult and thus leads to poor segmentation. To improve the segmentation accuracy, the contourlet transform is used for despeckling the ultrasound image followed by histogram equalization, and, thereafter, the horizontal and vertical scanline thresholding (HVST) method is employed for follicle detection using geometric parameters.

Contourlet transform : The first step of the algorithm is denoising the image, since ultrasound images are invariably noisy due to the mode of the image acquisition itself. (e.g. head of the

http://dx.doi.org/10.5772/56518

ultrasound device is not moist enough). Especially, a disturbing type of noise is the speckle noise. Therefore the more efficient speckle reduction method based on the contourlet transform is used for denoising medical ultrasound images [28]. The contourlets can be loosely interpreted as a grouping of nearby wavelet coefficients since their locaters are locally correlated due to smoothness of the boundary curve [29, 30]. The contourlet transform is a multiscale and multidirectional framework of discrete image [31]. It is the simple directional extension for wavelet that fixes its subband mixing problem and improves its directionality. In this transform, the multiscale and multidirectional analyses are separated in a serial way. The laplacian pyramid (LP), is first used to capture the point discontinuities followed by a directional filter bank (DFB) to link point discontinuities into linear structure. Thus, we perform a wavelet like transform for edge detection, and then a local directional transform for contour segment detection. In other words, the contourlet transform comprises a double filter bank approach for obtaining sparse expansions for typical images with contours.

The contourlet transform exploits smoothness of contour effectively by considering variety of directions following contour. The contourlet transform can be designed to be a tight frame along with thresholding in order to achieve denoising of the image more effectively. The algorithm for contourlet transform method is as follows [32,33] : Firstly, apply the log transform to the input ultrasound image. Then, apply the contourlet transform on the log transformed image upto n levels of Laplacian pyramidal decomposition and m directional decompositions at each level, where n and m depend on the image size. Next, perform thresholding of contourlet transformed image. Lastly, the despeckled image is obtained by performing inverse contourlet transform on the thresholded image. Then, histogram equalization is applied to enhance the contrast of the despeckled image.

i. Horizontal and Vertical Scanline (HVST) based method

Firstly, all the pixels which are darker than their neighborhood row wise (horizontal scan) and then column wise (vertical scan) is collected. Then, the two resultant images are added to yield a segmented image. The regions with area less than a threshold value are removed. The holes inside the region are filled. The nonzero pixels touching the image border are set to zero [34,35].

Horizontal Scanline Thesholding (HST) : The follicle region will have more or less same grey level value for all the pixels within it. The horizontal scanline thresholding method is described as follows; Consider the input image f of the size MxN. The sample mean m_i and standard deviation σ_i of the ith row subimage of f are given by the equations 9 and 10 :

$$m_i = \frac{1}{N}\sum_{j=1}^{N} f(i,j) \tag{9}$$

$$\sigma_i = \sqrt{\left(\frac{1}{N}\sum_{j=1}^{N}(f(i,j)-m_i)^2\right)} \tag{10}$$

Now, set T4 = m_i and T5 = σ_i. Then multiply T4 and T5 by positive scale factors K1 and K2 (empirically fixed). Binarize ith row subimage using the thresholds K1T4 and K2T5 separately. This procedure is carried out for the rows i=1,...,M and obtain the horizontal mean (standard deviation) thresholded image fhm (fhsd).

Vertical Scanline Thresholding (VST): The VST method is described as follows; Consider the input image f of the size MxN. The sample mean m_j and standard deviation σ_j of the jth column subimage are given by the equations 11 and 12:

$$m_j = \frac{1}{M}\sum_{i=1}^{M} f(i,j) \tag{11}$$

$$\sigma_j = \sqrt{\frac{1}{M}\sum_{i=1}^{M}(f(i,j) - m_j)^2} \tag{12}$$

Now, set T6 = m_j and T7 = σ_j. Then multiply T6 and T7 by positive scale factors K3 and K4 (empirically fixed), respectively. Binarize jth column subimage using thresholds K3T6 and K4T7 separately. This procedure is carried out for the columns j=1,...,N and obtain the vertical mean (standard deviation) thresholded image fvm (fvsd).

Image Fusion: The resultant images fhm and fvm are combined, to yield the image fhvm. Any region touching the borders are removed. The resultant images fhsd and fvsd are combined, to yield the image fhvsd. Any region touching the borders are removed. Finally, the resultant images fhvm and fhvsd are combined, to yield the segmented image fseg, which contains segmented regions in it. The regions in fseg having smaller area than the threshold T8 are removed. The regions are labeled (identified) and possible holes inside them are filled.

The geometric features are extracted and then 3σ-intervals around the mean are used for classification. The Table 2 shows the classification results of the HVST based method after ten-fold experiments for both the data sets D1 and D2. The average detection rates for the proposed Method I with D1 and D2 sets are 90.10% and 92.76%, false acceptance rates (FAR) are 11.71% and 9.89%, and false rejection rates (FRR) are 21.55% and 7.23%, respectively.

	Classification results for ten-fold experiments	
Data set	D1 set	D2 set
Classification rate	90.10%	92.76%
Type I error (FAR)	11.71%	21.55%
Type II error(FRR)	9.89%	7.23%

Table 2. Classification results of proposed method after ten-fold experiments.

ii. *Edge based method:* The edge based segmentation method, which is described in the section 2 (a), is applied to the histogram equalized image obtained after despeckling the input image using contourlet transform [36]. The follicle detection rate is improved in the edge based segmentation after applying contourlet transform and histogram equalization, as compared to the method in the section 2(a) which employs Gaussian low pass filter and edge based segmentation.

The HVST based method for the follicle detection is more effective as compared to edge based segmentation after applying contourlet transform and histogram equalization.

3. Active contour method for follicle detection

The active contour method is used for segmentation of ultrasound image to increase the follicle detection accuracy. Either 3σ intervals based classifier or fuzzy classifier may be employed for follicle detection.

i. Active contour method with 3σ intervals based classification

The follicle detection in ultrasound images of ovaries using active contour method uses the contourlet transform based method for preprocessing, active contour method for segmentation and 3σ-intervals around the mean for classification [37]. Initially, the input image is despekled by using the contourlet transform method. Next, histogram equalization is applied to enhance the contrast of the despeckled image. Further, the negative transformation is applied on the histogram equalized image [38], as the proposed segmentation method works on high intensity valued objects. In the segmentation stage, the active contour without edges method is used [39]. The resulting image after applying active contour method contains segmented regions with it. The geometric features are extracted and then 3σ-intervals around the mean is used for classification.

The Figure 5 (a) depicts sample original ultrasound image of the ovary. The resultant images obtained at different steps of the proposed method are shown in the Figure 5 (b)-(e). Many undesired spurious regions are also obtained (e.g., regions inside the endometrium). These spurious regions must be removed as much as possible. Therefore, the regions having an area less than T (empirical value) are removed (Figure 5(f)). The Figure 5(g) depicts the segmented follicles (outlined in white) superimposed on the original image. The Figure 5(h) depicts the recognized follicles after applying the classification rules and the Figure 5(i) shows the follicles annotated manually by the medical expert.

The Figure 6 depicts comparison of the active contour method with the HVST based segmentation method. In the Figure 6, (a) and (e) are two original images, while (b) and (f) are their corresponding segmented images by HVST method. Similarly, (c) and (g) are segmented images of active contour method. It is observed that the follicles, which were not detected by HVST based segmentation method (Figure 6 (b) and (f)), are correctly identified by the active contour method (Figure 6 (c) and (g)). The Figure 6 (d) and (h) show the manual segmentation rendered by the medical expert. Hence, the classification accuracy is improved in the active

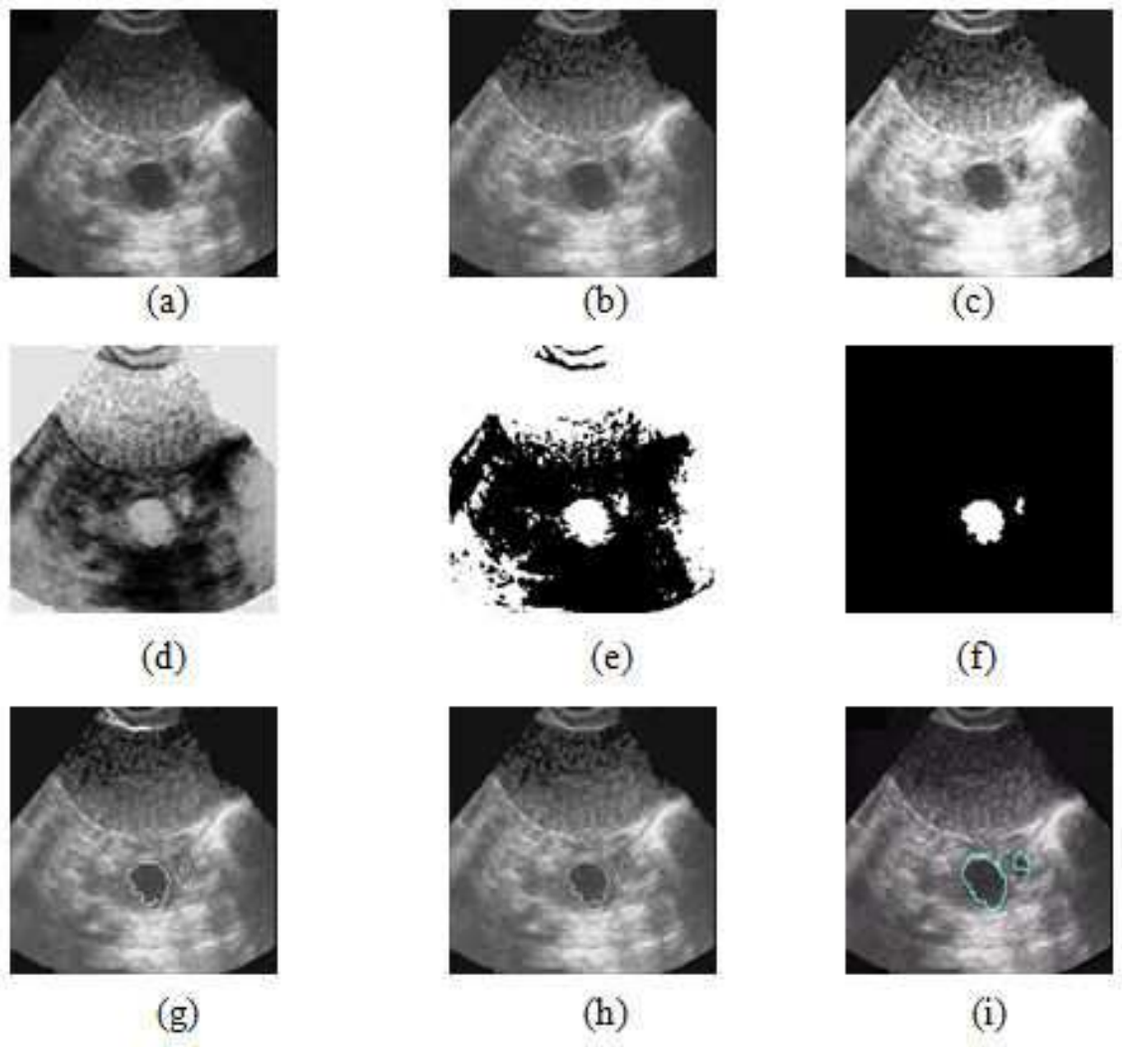

Figure 5. Original ultrasound image of the ovary and resultant images at different steps of proposed method. a) Original image, b) Contourlet transformed image (despeckling), c) Histogram equalized image, d) Image after applying negative transformation, e) Image after applying active contour without edges method, f) Segmented image after clearing the border, filling the holes and removing the small regions, g) Image showing recognized follicles(outlined in white) super imposed on the original image, h) Output image after classification, i) Manual segmentation of follicles by medical expert.

contour method as compared to HVST based segmentation method. The Table 3 presents the comparison of the experimental results of active contour method and HVST based method obtained for the original images in Figure 6. It is observed that the HVST based method leads to higher false acceptance rate (FAR) and false rejection rate (FRR). Further, the active contour method is found to yield more accurate results.

The Table 4 shows the comparison of classification results of the active contour method and the HVST based method after performing ten-fold experiments for both the data sets D1 and D2. The average detection rates for the active contour method using D1 and D2 sets are 92.3% and 96.66%, false acceptance rates (FAR) are 13.90% and 15.04%, and false rejection rates (FRR)

http://dx.doi.org/10.5772/56518

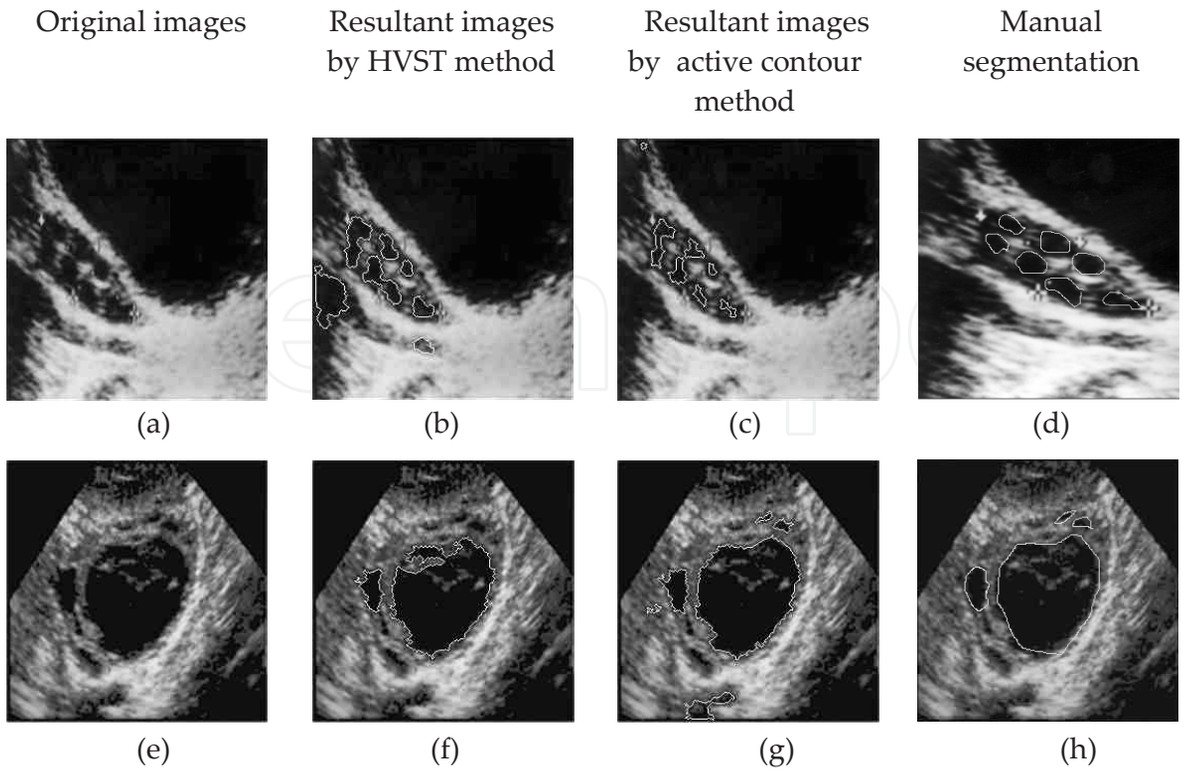

Figure 6. Comparison of resultant images of the active contour method with the HVST based method for two different original images. (a) and (e) original image, (b) and (f) resultant images of HVST method, (c) and (g) resultant images of the active contour method, (d) and (h) manual segmentation by medical expert.

Original Image	Number of follicles detected						
	Active contour method			HVST based method			Manual (by medical expert)
	Total	Correct	False	Total	Correct	False	
Figure 6 (a)	6	6	-	6	5	1	7
Figure 6 (e)	6	4	2	2	2	-	4

Table 3. Comparison of experimental results of active contour method and HVST based method for original images in Figure 6.

are 7.62% and 3.33%, respectively. The average detection rates for the HVST based method using D1 and D2 sets are 90.29% and 92.76%, false acceptance rates (FAR) are 14.10% and 21.55%, and false rejection rates (FRR) are 9.60% and 7.23%, respectively. Clearly, the method based on active contours outperforms the HVST based method.

	Classification results			
Data set	**D1 set**		**D2 set**	
Method	Active contour method	HVST based method	Active contour method	HVST based method Based Method
Classification rate	92.3%	90.29%	96.66%	92.76%
Type I error (FAR)	13.90%	14.10%	15.04%	21.55%
Type II error (FRR)	7.62%	9.60%	3.33%	7.23%

Table 4. Comparison of average classification results of the active contour method with the HVST based method after performing ten-fold experiments.

ii. Active contour method with fuzzy classification

To improve the performance of follicle detection in ultrasound images of ovaries, a new algorithm using fuzzy logic is developed. The method employs contourlet transform for despeckling, histogram equalization and negative transformation in the preprocessing step, the active contours without edges method for segmentation and fuzzy logic for classification. The seven geometric features are used as inputs to the fuzzy logic block of the Fuzzy Inference System (FIS). The output of the fuzzy logic block is a follicle class or non follicle class. The fuzzy-knowledge-base consists of a set of physically interpretable if-then rules providing physical insight into the process. The experimentation has been done using sample ultrasound images of ovaries and the results are compared with the inferences drawn by 3σ interval based classifier and also those drawn by the medical expert. The experimental results demonstrate the efficacy of the fuzzy logic based method [40].

Fuzzy set theory has been successfully applied to many fields, such as pattern recognition, control systems, and medical applications [41,42]. It has also been effectively used to develop various techniques in image processing tasks including ultrasound images [43]. The existence of inherent "fuzziness" in the nature of these images in terms of uncertainties associated with definition of edges, boundaries, and contrast makes fuzzy set theory an interesting tool for handling the ultrasound imaging applications [44]. Fuzzy logic was initiated in 1965 by L. A. Zadeh [45-48].

Training phase: The fuzzy inference system (FIS) of sugeno type is employed using the fuzzy input variables the ratio R of majoraxislength to minoraxislength, the compactness Cp, the circularity Cr, the tortuousity Tr, the extent E and the centriod C= (Cx, Cy) and output variables: follicle and non follicle classes. The Gaussian membership function is used for each of the fuzzy input variables with mean and standard deviation of the corresponding variables. Let mfr, mfcp, mfcr, mftr, mfe, mfcx and mfcy be the Gaussian membership functions of the fuzzy input variables R, Cp, Cr, Tr, E and C=(Cx,Cy), respectively, belonging to the follicle class. Let mfr1, mfcp1, mfcr1, mftr1, mfe1, mfcx1 and mfcy1 be the Gaussian membership functions of these input variables belonging to the non-follicle class.

http://dx.doi.org/10.5772/56518

During the training phase, the geometrical features, namely, R, Cp, Cr, Tr, E and C=(Cx,Cy), are computed for regions known to be follicles in the training images in consultation with the medical expert. Then, the mean and standard deviation of each of the geometric parameters R, Cp, Cr,Tr, E and C=(Cx,Cy), are computed which are used to set the rules for classification of follicles. The mean and standard deviation of these parametric values are stored as knowledge base which is shown in the Table 5. These values are used as the pattern (parameters) in FIS membership function design.

	Mean value	**Standard deviation**
Ratio(R)	1.82	0.58
Compactness (C_p)	37.35	10.16
Circularity (C_r)	0.37	0.09
Tortousity (T_r)	0.27	0.03
Extent (E)	0.51	0.09
Centriod C=(Cx,Cy)	(251, 55)	(201,70)

Table 5. The knowledge base of mean and standard deviation of parametric values of geometric features or the follicle regions

The construction of the membership functions for the output variables is done in the similar manner. Since this is Sugeno-type inference (precisely, zero-order Sugeno), constant type of output variable fits the best to the given set of outputs (1 for follicle and 0 to non-follicle classes). Based on the descriptions of the inputs (the ratio R of majoraxislength to minoraxislength, the compactness Cp, the circularity Cr, the tortousity Tr, the extent E and the centriod C=(Cx,Cy)) and output variables (follicle and non follicle). The fuzzy rules for classification procedure in verbose format are as follows:

i. IF (R is input to mfr) AND (Cp is input to mfcp) AND (Cr is input to mfcr) AND (Tr is input to mftr) AND (E is input to mfe) AND (Cx is input to mfcx) AND (Cy is input to mfcy) THEN (class is follicle)

ii. IF (R is input to mfr1) AND (Cp is input to mfcp1) AND (Cr is input to mfcr1) AND (Tr is input to mftr1) AND (E is input to mfe1) AND (Cx is input to mfcx1) AND (Cy is input to mfcy1) THEN (class is non-follicle).

At this point, the fuzzy inference system has been completely defined, in that the variables, membership functions and the rules necessary to determine the output classes are in place.

Testing phase: During the testing phase, the geometric features R, Cp, Cr, Tr, E and C= (Cx, Cy) are computed for each segmented region of the input image and then the above fuzzy classification rules are applied to determine whether the region is a follicle or not a follicle.

Experimental results: The ten-fold experiments are performed for the classification and the average follicle detection rate is computed. The Figure 7 (a) depicts an original ultrasound

image of the ovary and the resultant images at different steps of fuzzy based method are shown in Figure 7(b)-(e). Many undesired spurious regions are also obtained (e.g., regions inside the endometrium). These spurious regions must be removed as much as possible. Therefore, the regions having an area less than T are removed (Figure 7(f)). The Figure 7 (g) depicts the segmented follicles (outlined in white) superimposed on the original image. The Figure 7 (h) depicts the recognized follicles after applying classification rules and Figure 7 (i) shows the follicles annotated manually by the medical expert.

The Figure 8 depicts comparison of the fuzzy logic based classification with the 3σ intervals based classification [section 3(i)]. In the Figure 8 (a) and (d) are two original images, (b) and (e) are their corresponding resultant images by the 3σ intervals based method. and, (c) and (f) are resultant images of fuzzy based method. It is observed that the regions which are misclassified as follicles, by the method in [section 3(i)] (Figure 8 (b) and (e)), are correctly classified by the fuzzy logic based method (Figure 8 (c) and (f)). Hence, the classification accuracy of the fuzzy logic based method is improved as compared to the method in [section 3(i)]. The Table 6 presents number of follicles detected in the results of the fuzzy based method and the method in [section 3(i)] corresponding to the original images in the Figure 8.

	Number of follicles detected						
Method	**fuzzy based method**			**3σ intervals based method [section 3(i)]**			**Manual (by medical expert)**
Input original image	Total	Correct	False	Total	Correct	False	
Figure 8(a)	3	3	-	5	3	2	3
Figure 8(d)	1	1	-	3	1	2	1

Table 6. Comparison of experimental results of proposed fuzzy logic based classification and 3σ interval based classification based method for original images in the Figure 8.

The Table 7 shows the comparison of classification results of fuzzy based method and the method in [section 3(i)] after ten-fold experiments for both the data sets. The average detection rates for the fuzzy based method with D1 and D2 sets are 98.18% and 97.61%, false acceptance rates (FAR) are 4.52% and 9.05%, and false rejection rates (FRR) are 1.76% and 2.37%, respectively. The average detection rates for the method in the Section 3(i) with D1 and D2 sets are 92.3% and 96.66%, false acceptance rates (FAR) 13.6% and 15.04%, and false rejection rates (FRR) are 7.62% and 3.33%, respectively. It is observed that the false acceptance rate (FAR) is reduced and the classification accuracy is improved in case of the fuzzy logic based method as compared to that in the 3σ intervals based method [section 3(i)] for classification.

http://dx.doi.org/10.5772/56518

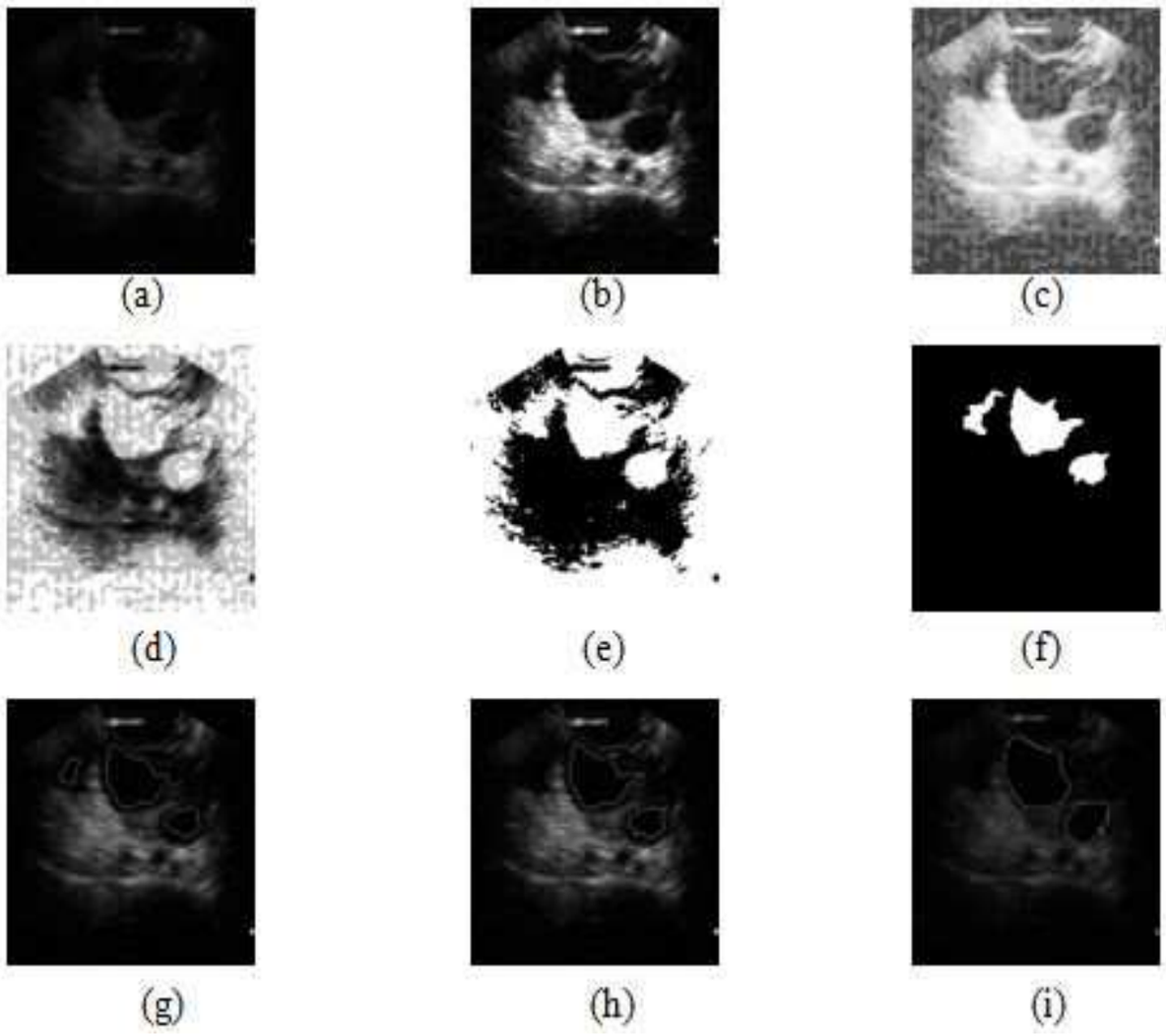

Figure 7. Original ultrasound image of the ovary and resultant images at different steps of fuzzy based method. a) Original image, b) Contourlet transformed image (despeckling), c) Histogram equalized image, d) Image after applying negative transformation, e) Image after applying active contour without edges method, f) Segmented image after clearing the border, filling the holes and removing the small regions, g) Image showing recognized follicles(outlined in white) super imposed on the original image, h) Output image after fuzzy classification, i) Manual segmentation of follicles by medical expert.

4. Ovarian classification

The ovaries are classified into three types based on the number and size of the follicles. Ovary is scanned, follicles are identified by using the method described the section 3, and the size of the follicles are measured and the number of follicles are counted.

There are three categories :

- The ovary containing 1-2 follicles with size measuring greater than 28mm in size, is a cystic ovary.

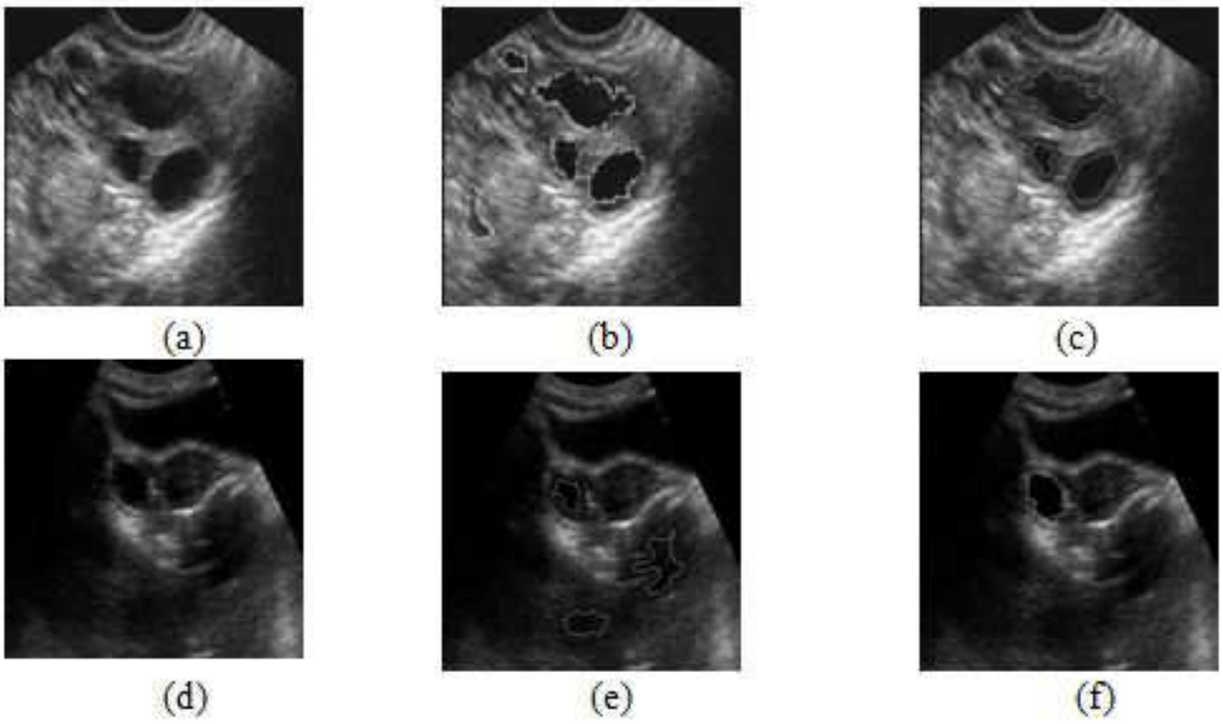

Figure 8. Comparison of resultant images of the fuzzy based method with the 3σ intervals based classification for two different original images. (a) and (d) original images, (b) and (e) resultant images of 3σ intervals based, (c) and (f) resultant images of fuzzy based method.

- The ovary containing 12 or more follicles with size measuring less than 10mm, is a polycystic ovary.
- The ovary containing 1-10 follicles with size measuring 2-10mm, are antral follicles and with the 10-28mm size, are dominant follicles, is a normal ovary with m number of antral follicles and n number of dominant follicles.

The two ovarian classification methods are discussed below [Hiremath and Tegnoor, 2012]:

i. Fuzzy ovarian classification

Training phase: The fuzzy inference system (FIS) of sugeno type is employed using the fuzzy input variables the number of follicles NN and the size of the follicle S and output variables: normal, cystic and polycystic ovarian classes. The Trapezoidal membership function is used for each of the fuzzy input variables with minimum and maximum value of the corresponding variables. Let mfn1 and mfs1, mfn2 and mfs2, and mfn3 and mfs3, be the trapezoidal membership functions of the fuzzy input variables NN and S respectively, belonging to the normal ovarian class, cystic ovarian class, polycystic ovarian class.

During the training phase, the parameters, namely, NN and S, are computed for the ovarian images known to be healthy, cystic and polycystic ovary in the training images in consultation with the medical expert, which are used to set the rules for classification of ovarian images.

We denote,

http://dx.doi.org/10.5772/56518

n1 - number of follicles of normal ovary

sz1 - size of the follicles in the normal ovary

n2 - number of follicles of cystic ovary

sz2- size of the follicles in the cystic ovary

n3 - number of follicles of polycystic ovary

sz3 - size of the follicles in the polycystic ovary

The number of follicles and size of follicles of these three classes are stored as knowledge base which is shown in the Table 8.

	Classification results			
Data set	**D1 set**		**D2 set**	
Methods	Fuzzy logic method	3σ interval based method [section 3(i)]	Fuzzy logic method	3σ interval based method [section 3(i)] Based Method
Classification rate	98.18 %	92.3 %	97.61%	96.66%
Type I error (FAR)	4.52 %	13.6 %	9.05%	15.04%
Type II error (FRR)	1.76 %	7.62 %	2.37 %	3.33 %

Table 7. Comparison of classification results of fuzzy based classification method with 3σ intervals based method after ten-fold experiments.

The construction of the membership functions for the output variables is done in the similar manner. Since this is Sugeno-type inference (precisely, zero-order Sugeno), constant type of output variable fits the best to the given set of outputs (0 for normal ovary and 0.5 for cystic ovary and 1 for polycystic ovary). Based on the descriptions of the inputs (the number of the follicles NN and size of the follicles S) and output variables (normal ovary, cystic ovary, polycystic ovary). The fuzzy rules for classification procedure in verbose format are as follows:

i. IF (n1 is input to mfn1) AND (sz1 is input to mfs1) THEN (class is normal ovary)

ii. IF (n2 is input to mfn2) AND (sz2 is input to mfs2) THEN (class is cystic ovary)

iii. IF (n2 is input to mfn3) AND (sz3 is input to mfs3) THEN (class is polycystic ovary)

At this point, the fuzzy inference system has been completely defined, in that the variables, membership functions and the rules necessary to determine the output classes are in place.

Image type	Number of follicles	Size of the follicle
Normal ovary	1-10	15-10000
Cystic ovary	1-2	4300-75000
Polycystic ovary	12-20	15-9000

Table 8. The knowledge base of number of follicles and size of follicles of all the three classes

Testing phase: During the testing phase, we compute the number of follicles NN, and the size of each follicle S, for an ovary with the detected follicles and apply the above classification rules to determine whether an ovary is normal, cystic, and polycystic.

Experimental results: The experimentation is done using image data set D3. The D3 set consists of 70 sample ultrasound ovarian images of size 512x512, out of which 35 images are used for training and 35 for testing. In the first step, the ten-fold experiments for the follicle detection are done and then the average follicle detection rate is computed. Further, in the second step, for the ovary classification, 70 sample images of the detected follicles are used, of which 35 are used for training and 35 are used for testing. The ten-fold experiments for the ovarian classification are done and the average classification rate for the ovarian type is computed. The Figure 9 shows the sample results for the ovarian classification method. detection method after performing ten-fold experiments for the image data set. The Table 9 shows the average classification results of follicle detection method after performing ten-fold experiments for the image data set. The follicle detection method (Section 3(ii)) yields the average detection rate for the fuzzy based method 98.47%, false acceptance rate (FAR) 2.61% and false rejection rate (FRR) 1.47%.

Classification rate	Type I error (FAR)	Type II error (FRR)
98.47%	2.61%	1.47%

Table 9. Average classification results after ten-fold experiments

The Table 10 shows the ten-fold experimental results of the ovarian classification based on fuzzy inference rules. It is observed that the average normal ovary cyst ovary and polycystic ovary is 100%, with zero false acceptance rate is (FAR) and false rejection rate (FRR). Although, the proposed ovarian classification method yields 100% classification results, it is to be noted that these results are with reference to the limited data set used for experimentation. However, in case of different data sets, with varying image resolution, image sizes and numbers, the classification accuracy may be less than 100%.

http://dx.doi.org/10.5772/56518

Ovarian class	Number of images	Number of correctly classified images	Manual detection	Type I error	Type II error
Normal ovary	15	15	15	-	-
Cystic ovary	10	10	10	-	-
Polycystic ovary	10	10	10	-	-

Table 10. Experimental results for classification accuracy for all the three classes

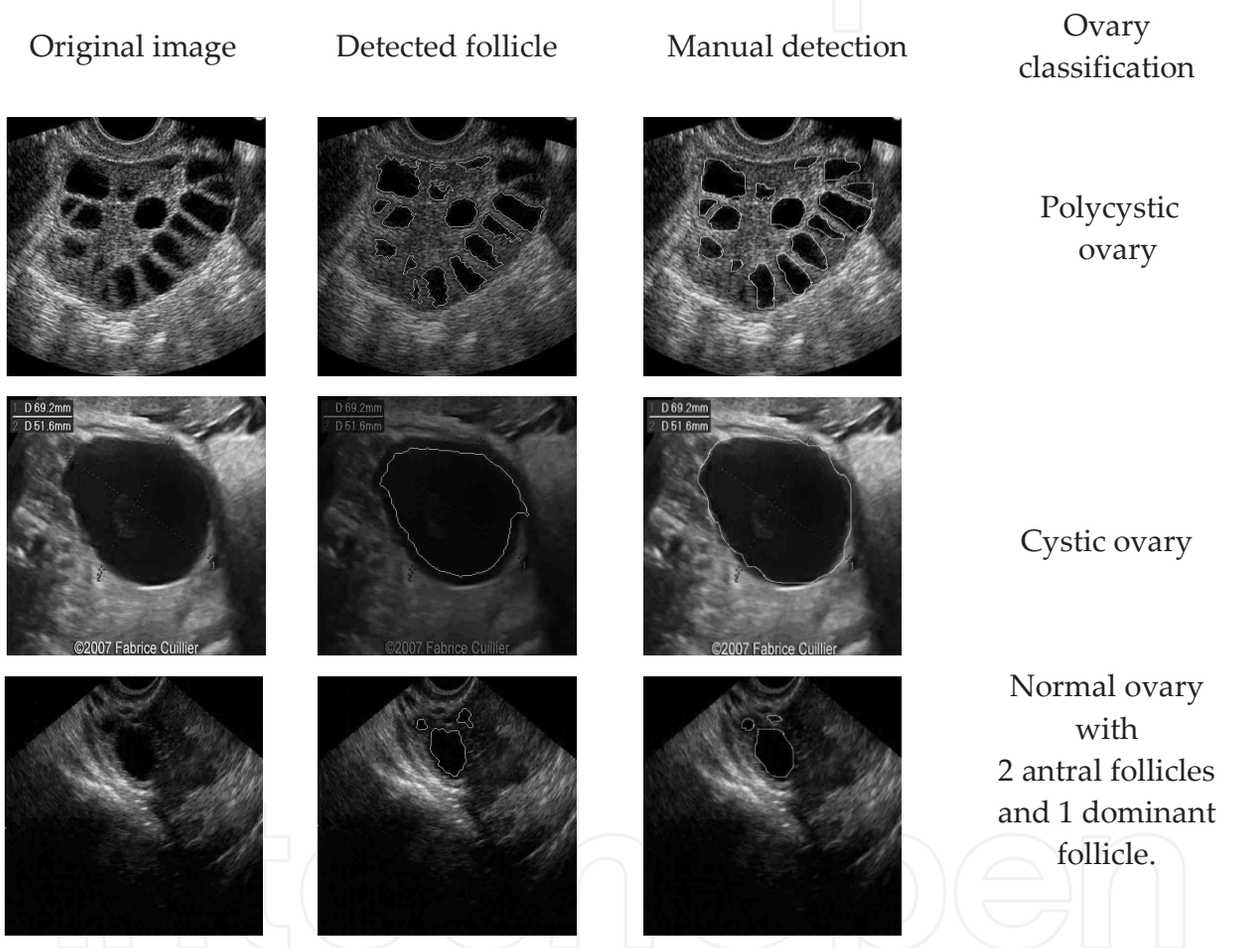

Figure 9. Sample results for proposed ovarian classification method

ii. Ovarian classification by using SVM

The aim of support vector machine (SVM) is to devise a computationally efficient way of learning separating hyper planes in a high dimensional feature space [49]. The SVMs have been shown to be an efficient method for many real-world problems because of its high generalization performance without the need to add a priori knowledge. Thus, SVMs have much attention as a successful tool for classification [50,51], image recognition [52,53] and

bioinformatics [54]. The SVM model can map the input vectors into a high-dimensional feature space through some non-linear mapping, chosen a priori. In this space, an optimal separating hyperplane is constructed. SVM is the implementation of the structural risk minimization principle whose object is to minimize the upper bound on the generalization error. Given a set of training vectors (l in total) belonging to separate classes, (x1, y1), (x2, y2), (x3, y3),..., (xl, yl), where $x_i \in R^n$denotes the ith input vector and $y_i \in \{+1, -1\}$ is the corresponding desired output. The maximal margin classifier aims to find a hyperplane w: wx + b = 0 to separate the training data. In the possible hyperplanes, only one maximizes the margin and the nearest data point of each class. The Figure 10 shows the optimal separating hyperplane with the largest margin. The support vectors denote the points lying on the margin border. The solution to the classification is given by the decision function in the equation 13.

$$f(x) = sign\left(\sum_{i=1}^{N_{SV}} \alpha_i y_i k(s_{i,} x) + b\right) \tag{13}$$

where $\alpha_i$is the positive Lagrange multiplier, s_i is the support vector (N_{SV} in total) and k(s_i, x) is the function for convolution of the kernel of the decision function. The radial kernels perform best in our experimental comparison, and, hence, are chosen in the proposed diagnosis system. The radial kernels are defined as (equation 14).

$$k(x, y) = \exp\left(-\gamma\left(x - y\right)^2\right) \tag{14}$$

By using the SVM method, firstly, follicles are detected and secondly, the ovarian classification is performed [55]. During the training phase, the parameters, namely, the number of follicles NN and the size of the follicle S, are determined for the ovarian images known to be normal, cystic and polycystic ovary in the training images in consultation with the medical expert. The quadratic kernel is used for training the three-class SVM classifier; normal, cystic and polycystic ovary being the three classes.

During the testing phase, the parameters, namely, the number of follicles NN and the size of follicles S, are determined, and then, the SVM classifier is used to determine whether an ovary is normal, cystic, or polycystic.

Experimental results: The Table 11 shows the comparison of classification results of SVM based method and the fuzzy based method in [section 4(i)] after ten-fold experiments. The average follicle detection rate for the SVM method is 98.89%, false acceptance rate (FAR) is 1.61 % and false rejection rate (FRR) is 1.10%. The average detection rate for the method in [section 4(i)] is 98.47%, false acceptance rate (FAR) is 2.61% and false rejection rate (FRR) is 1.47%. It is observed that the classification accuracy is improved in the SVM based method as compared to the fuzzy based method [section 4(i)].

http://dx.doi.org/10.5772/56518

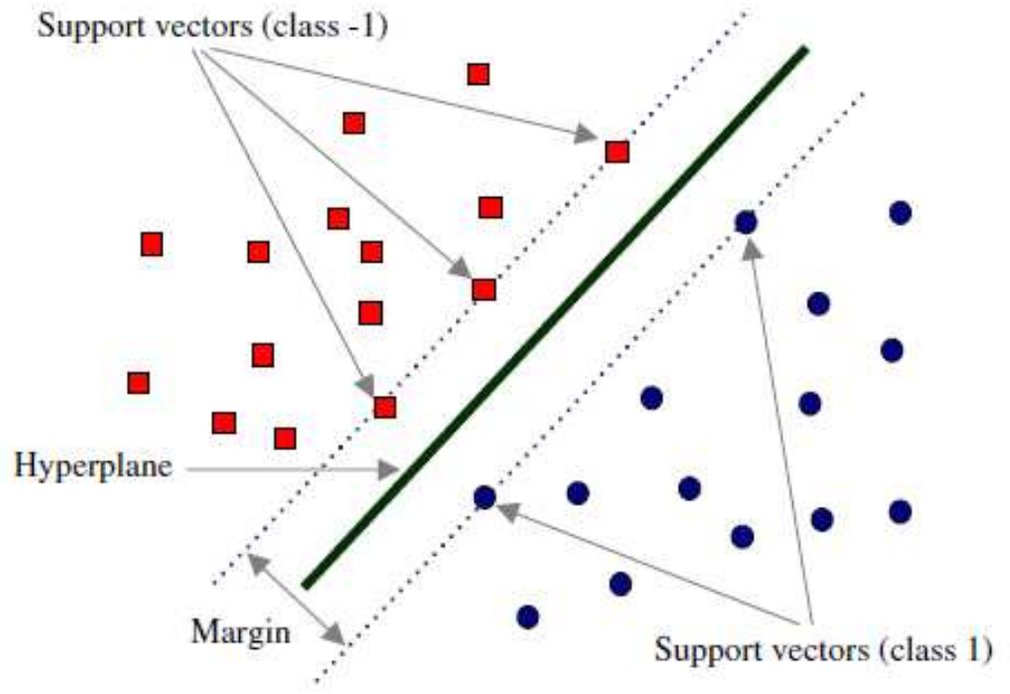

Figure 10. Optimal hyperplane for support vector machine

	Classification accuracy (%) of follicle detection	
Method	**SVM based method**	**Fuzzy based method [4(i)]**
Classification rate	98.89 %	98.47%
Type I error (FAR)	1.61 %	2.61%
Type II error (FRR)	1.10 %	1.47%

Table 11. Comparison of classification results of SVM based method and fuzzy based method [section 4(i)] for follicle detection after ten-fold experiments

The Table 12 shows the ten-fold experimental results of the ovarian classification based on SVM. It is observed that the average classification rates for normal ovary, cystic ovary and polycystic ovary are 100%, with zero false acceptance rate (FAR) and zero false rejection rate (FRR). It is observed that both the proposed SVM based method and the fuzzy based method [section 4(i)] yield 100% accuracy in ovarian classification, although the SVM outperforms the fuzzy method [section 4(i)] in follicle detection.

The Table 13 shows the comparison of all the follicle detection and ovarian classification methods developed in the present study and the other follicle detection methods available in the literature.

Ovary type	Number of images	Number of correctly classified images		Manual detection by expert	Type I error (FAR)		Type II error (FRR)	
		SVM	Fuzzy [4(i)]		SVM	Fuzzy [4(i)]	SVM	Fuzzy [4(i)]
Normal ovary	15	15	15	15	0	0	0	0
Cystic ovary	10	10	10	10	0	0	0	0
Polycystic ovary	10	10	10	10	0	0	0	0

* Type I Error: Regions are not follicles, but they are recognized as follicles.

**Type II Error: Regions are follicles, but they are not recognized as follicles.

Table 12. Experimental results for classification accuracy of the SVM based method for the three classes of ovaries in comparison with the fuzzy based method [section 4(i)]

Method	Data set used	Classification accuracy
Edge based method with Gaussian lowpass filter	D1	62.3%
	D2	45.2%
Watershed segmentation method	D1	49.55%
	D2	50.68%
Optimal thresholding method with Sobel operator	D1	50.77%
	D2	61.82%
HRGMF based thresholding method	D1	79.47%
	D2	68.86%
Edge based method with contourlet transform method	D1	75.2%
	D2	59.95%
HVST based method	D1	90.10%
	D2	92.76%
Active contour with 3σ interval based method	D1	92.37%
	D2	96.66%
Active contour with fuzzy classification	D1	98.18%

Method	Data set used	Classification accuracy
	D2	97.61%
Active contour with fuzzy classification of ovary	D3	98.47%
Active contour with SVM classification of ovary	D3	98.47%
Modified region growing and LD classifier [Maryruth et al., 2007]	(70)	83.25%
Region growing method [Potocnik and Zazula, 2000]	(50)	78%
Cellular neural network [Cigale and Zazula, 2000]	(50)	60%
Edge based method [Potocnick et al., 2002]	(50)	61%
Prediction based method [Potocnick and Zazula, 2002]	(50)	78%

Note : D1, D2 and D3 are image data sets.

Table 13. Comparison of the proposed method with all the other methods proposed in the present study and also with the other methods in the literature.

5. Conclusion

The main significant research contributions that fulfill the objectives set in the present chapter are :

i. Automatic detection of follicles using better segmentation and classification methods.

ii. Automatic ovarian classification into three categories, namely: normal ovary, cystic ovary and polycystic ovary.

The performance comparison of the various methods proposed in the present study and other methods in the literature is summarized in the Table 13. It is observed that :

i. the proposed method using contourlet transform based despeckling, active contour without edges based segmentation, geometric feature extraction and fuzzy logic or SVM based classifier, has yielded better follicle detection results; and,

ii. the proposed method for ovarian classification using fuzzy or SVM has yielded better classification results.

These research contributions are expected to be useful for the design and development of the software tool to support the medical experts, namely, Gynecologists and Radiologists, in their effort for ovarian image analysis and to implement the same in automated diagnostic systems. Further, these research contributions serve as the basis for design of automatic systems for the detection of the follicles inside the ovary under the examination during the entire female cycle and to study the ovarian morphology and, thus, help the medical experts for monitoring follicles and identifying the ovarian type during the course of infertility treatment of patients. The burden of the experts is significantly reduced in their everyday routine, without sacrificing the accuracy of diagnosis and prognosis.

The future research in this direction would be to take up the analysis of ovarian images captured at regular intervals for various subjects undergoing drug susceptibility tests. Further, the image processing methods could be developed in the detection of ovarian cancer stages.

Acknowledgements

Authors are thankful to Mediscan Diagnostics Care, Gulbarga, for providing the ultrasound images of ovaries. We are indebted to Dr. Suchitra C. Durgi, Radiologist, Dr. Chetan Durgi, Radiologist and Dr. Suvarna M. Tegnoor, Gynaecologist, Gulbarga, for helpful discussions and for rendering manual detection of follicles and ovarian classification in ultrasound images of ovaries.

Author details

P. S. Hiremath* and Jyothi R. Tegnoor*

*Address all correspondence to: hiremathps53@yahoo.com

*Address all correspondence to: jyothi_rt1@yahoo.co.in

Dept of Computer Science, Gulbarga University, Gulbarga, India

References

[1] Gougeon A. and Lefevre B. Evolution of the Diameters of the Largest Healthy and Atretic Follicles During the Human Menstrual Cycle, Reproduction and Fertility 1983;69: 497-502.

[2] Gougeon A., Adashi E. and Leung P. Dynamics of Human Follicular Growth, a Morphologic Perspective: Comprehensive Endocrinology, The Ovary, Raven Press, New York, 1993: 21-39.

[3] Pellicer A., Gaitán P., Neuspiller F., Ardiles G., Albert C., Remohí J. and Simón C., Ovarian Follicular Dynamics: From Basic Science to Clinical Practice, Journal of Reproductive Immunology 1998; 39(1-2) 29-61.

[4] Hanna M. D., Chizen D. R. and Pierson R. Characteristics of Follicular Evacuation During Human Ovulation, J Ultrasound Obstet Gynaecol 1994; 4(6) 488-493.

[5] Pierson R. and Chizen D. Ultrasonography of Normal and Aberrant Ovulation. Imaging in Infertility and Reproductive Endocrinology, 1994;155-166.

[6] Bal A. and Mohan H. Malignant Transformation in Mature Cystic Teratoma of the Ovary: Report of Five Cases and Review of the Literature, Arch Gynecol Obstet, 2007; 275(3)179-182.

[7] Yamanaka Y. and Tateiwa Y. Preoperative Diagnosis of Malignant Transformation in Mature Cystic Teratoma of The Ovary, Eur J Gynaecol Oncol 2005; 26(4)391-392.

[8] Battaglia C., Artini P. G., Genazzani A. D., Gremigni R., Slavatori M. R. and Sgherzi M. R., Color Doppler Analysis in Oligo and Amenorrheic Women with Polycystic Ovary Syndrome. Gynecolog Endocrinto, 1997;11:105-110.

[9] Balen Adam H., Joop S. E. Laven, Seang-Lin Tan and Didier Dewailly, Ultrasound Assessment of the Polycystic Ovary: International Consensus Definitions, Human Reproduction, 2003;9(6)505-511.

[10] Pache T. D., Wladimiroff J. W., Hop W. C. and Fauser B. C. How to Discriminate Between Normal and Polycystic Ovaries: Transvaginal US Study. Radiology 1992;183(2) 421-423.

[11] Kelsey T.W. and Wallace W. H. B. Ovarian Volume Correlates Strongly with Number of Non Growing Follicles in the Human Ovary, Obstretics and Gynocology International, 2012; Article-id 305025.

[12] Potocnik B., Zazula D., Korze D. Automated Computer-Assisted Detection of Follicles in Ultrasound Images of Ovary. Journal of Medical Systems 1997; 21(6) 445-457.

[13] Potocnik B., Viher B. and Zazula D. Computer assisted detection of ovarian follicles based on ultrasound images, Proc. of a szamitastechnika orvosies biological alkalmazasai, Verzprem, Hungary, pp. 24-34; 1998.

[14] Potocnik B. and Zazula D. Aktivne krivulje-nadgradnja razpoznavalnih sistemov (Active contours-an extension of recognition systems). Proceedings of 7th Electrotechnical and Computer Science Conference ERK 98, Portoroz, Slovenia, Vol. B, 1998; 249-252.

[15] Potocnik B. and Zazula D. Automated Analysis Of Sequence of Ovarian Ultrasound Images, Part I: Segmentation of Single 2D Images. Image Vision and Computing 2002; 20(3) 217-225.

[16] Sarty G. E., Liang W., Sonka M. and Pierson R. A. Semiautomated Segmentation of Ovarian Follicular Ultrasound Images Using a Knowledge Based Algorithm. Ultrasound in Medicine and Biology, 1998; 24(1)27-42.

[17] Cigale B. and Zazula D. Segmentation of Ovarian Ultrasound Images Using Cellular Neural Networks, International Journal of Pattern Recognition and Artificial Intelligence, 2004; 18, 563-581.

[18] Krivanek and Sonka M. Ovarian Ultrasound Image Analysis Follicle Segmentation. IEEE Transactions on Medical Imaging, 1998; 17(6) 935-944.

[19] Maryruth, Lawrence J. and Eramian Mark G. Computer Assisted Detection of Polycystic Ovary Morphology, Ultrasound Images 2007; 23(2) 306-309.

[20] Mehrotra P., Chakraborthy C., Ghoshdastidar B. and Ghostidas S. Automated Ovarian Follicle Detection for Polycystic Ovarian Syndrome, Proc. of IEEE International Conference on Image Information Processing (ICIIP), 3-5 Nov 2011, Himachal Pradesh, India, 1-4; 2011.

[21] Hiremath P. S. and Tegnoor J. R. Automatic Detection of Follicles in Ultrasound Images of Ovaries, Proc. of Second International Conference on Cognition and Recognition (ICCR-08), 15-17 Apr. 2008, Mysore, India, pp 468-473; 2008.

[22] Hiremath P. S. and Tegnoor J. R. Automatic Detection of Follicles in Ultrasound Images of Ovaries, Proc. of Third International Conference on Systemic, Cybernetics and Informatics (ICSCI-09), 07-10 Jan. 2009, Hyderabad, India, pp. 327-330; 2009.

[23] Hiremath P. S. and Tegnoor J. R. Automatic Detection of Follicles in Ultrasound Images of Ovaries by Optimal Threshoding Method, International Journal of Computer Science and Information Technology 2010; 3(2) 217-220.

[24] Gonzalez R. C. and Woods R. E. Digital Image Processing, Second Edition, Pearson Edu; 2002.

[25] Jing Hanm B S., Shin D. V., Arthur G. L. and Chi-Ren Shyu, 2010, Multiresolution Tile Based Follicle Detection Using Colour and Textural Information of Follicular Lymphoma IHC Slides, Proc. of IEEE International Conference on Biomedicine Workshop., 18-21 Dec. 2010, Hong Kong, China, pp. 886-87; 2010.

[26] Hiremath P. S. and Tegnoor J. R. Automatic Detection of Follicles in Ultrasound Images of Ovaries using HRGMF Based Segmentation, International Journal of Multimedia, Computer Vision and Machine Learning (IJMCVML) 2010; 1(1) 83-87.

[27] Koo Ja. I. and Song B. Park. Speckle Reduction with Edge Preservation, Medical Ultrasonics 1991; 3(13) 211-237.

[28] Srinivasrao Ch., Srinivaskumar S. and Chattergi B. N. Content Based Image Retrieval Using Contourlet Transform, ICGST-GVIP Journal 2007;7(3) 9-15.

[29] Jainping Zhou, Arthur L. Cunha and Minh N. Do, Non subsampled Contourlet Transform: Construction and Application in Enhancement, Proc. of IEEE International Conference on Image Processing, 11-14 Sept. 2005, Genoa, Italy, pp. 469-72; 2005.

[30] Do Minh N. and Vetterli Martin, The Contourlet Transform: An Efficient Directional Multiresolution Image Representation, IEEE Transaction on Image Processing 2005; 14(12)2091-2106.

[31] Eslami Ramin and Hayder Radha, 2006, Translation invariant contourlet transform and its application image denoising, IEEE Transactions on Image Processing 2005;15(11) 3362-74.

[32] Hiremath P. S., Akkasaliger P. and Badiger S., 2009, Despeckling medical ultrasound images using the contourlet transform, Proc. of Indian International Conferance on Artificial Intelligence, 16-18 Dec. 2009, Tumkur, India, pp. 1814-1827.

[33] Hiremath P. S., Akkasaliger P. and Badiger S., Performance Comparision of Wavelet Transform and Contourlet Transform Based Method for Despekling Medical Ultrasound Images, International Journal of Computer Applications, 2011, 26(9)34-41.

[34] Hiremath P. S. and Tegnoor J. R. Automatic Detection of Follicles in Ultrasound Images of Ovaries using Horizontal and Vertical Scanline Thresholding Method, Proc. of Second International Conference on Signal and Image Processing (ICSIP-09), 12-14 Aug. 2009, Mysore, India, pp 468-473;2009.

[35] Hiremath P. S. and Tegnoor J. R. Recognition of Follicles in Ultrasound Images of Ovaries using Geometric Features, Proc. of Second IEEE International Conference on Biomedical and Pharmaceutical Engineering (ICBPE-09), 2-4 Dec. 2009, Singapore, ISBN 978-1-4244-4764-0/09; 2009.

[36] Hiremath P. S. and Tegnoor J. R. Automatic Detection of Follicles in Ultrasound Images of Ovaries using Edge based Method, International Journal of Computer Applications (IJCA), Special Issue on "Recent Trends in Image Processing and Pattern Recognition", RTIPPR, pp 120-125, ISSN 0975-8887; 2010.

[37] Hiremath P. S. and Tegnoor J. R. Automatic Detection of Follicles in Ultrasound Images of Ovaries using Active Contours Method, International Journal of Service Computing and Computational Intelligence (IJSCCI) 2011; 1(1) pp 26-30, ISSN 2162-514X.

[38] Jahne B., Digital Image Processing. Berlin, Germany Springer–Verlag; 1993.

[39] Chan Tony F. and Vese Luminita A., Active Contours Without Edges, IEEE Transactions on Image Processing 2001; 10(2) 266-277.

[40] Hiremath P. S. and Tegnoor J. R. Fuzzy Logic Based Detection of Follicles in Ultrasound Images of Ovaries, Proc. of Fifth Indian International Conference on Artificial

Intelligence (IICAI-2011), 14-16 Dec 2011, Tumkur, Karnataka, India, pp 178-189, ISBN: 978-0-9727412-8-6; 2011.

[41] Sourabh Dash, Raghunathan Rengaswamy and Venkat Subramanian. Fuzzy-Logic Based Trend Classification for Fault Diagnosis of Chemical Processes, International Journal of Computers and Chemical Engineering 2003; 27(3)347-362.

[42] Nedeljkovic I., Image Classification Based on Fuzzy Logic, The International Archives of the Photogrammetry, Remote Sensing and Spatial Information Sciences 2004, 34: 173-179,

[43] Kerre E. E. and Nachtegael M. Fuzzy Techniques in Image Processing. Springer, Heidelberg; 2000.

[44] Khademi A., Sahba F., Venetsanopoulos A. and Krishnan S., 2009, Region, Lesion and Border-Based Multiresolution Analysis of Mammogram Lesions, Proc. of the Sixth International Conference on Image Analysis and Recognition (ICIAR), 6-8 July 2009, Halifex, Canada, pp. 802-813.

[45] Zadeh L. A. Fuzzy Sets, Information and Control,1965; 8: 333-335.

[46] Zadeh L.A. Outline of a New Approach to the Analysis of Complex Systems and Decision Processes, IEEE Transactions on Systems, Man, and Cybernatics 1973; 3(1).

[47] Zadeh L.A. Fuzzy algorithms, Info and Ctl. 1968, 12: 94-102.

[48] Zadeh L.A. Making Computers Think Like People, IEEE. Spectrum 1984; pp. 26-32.

[49] Christianini N. and Shawe-Taylor J. An Introduction to Support Vector Machines and Other Kernel-Based Learning Methods. Cambridge University Press, UK 12; 2000.

[50] Kim K. I., Jung K., Park S. H. and Kim H. J. Support Vector Machines for Texture Classification, IEEE Trans Pattern Anal Mach Intell 2002; 24(11) 1542-1550.

[51] Song Q., Hu W. J. and Xie W. F., 2002, Robust Support Vector Machine With Bullet Hole Image Classification, IEEE Trans. Systems, Man and Cybenetics, Part C: Applications and Review 2002; 32(4) 440-448.

[52] El Naqa I., Yang Y. Y., Wernick M. N., Galatsanos N. P. and Nishikawa R. M. A Support Vector Machine Approach for Detection of Micro Calcifications. IEEE Trans Med Imaging 2002; 21(2)1552-1563.

[53] Yang M. H., Roth D. and Ahuja N. A tale of two classifiers: SNoW vs. SVM in visual recognition, Proc. of Seventh European Conference on Computer Vision, Copenhagen, Denmark, 27 May-2 June 2002, pp. 688-699; 2002.

[54] Sun Y. F., Fan X. D. and Li Y. D., Identifying Splicing Sites in Eukaryotic RNA: Support Vector Machine Approach, Comput. Biol. Med 2003, 33(1)17–29.

[55] Hiremath P. S. and Tegnoor J. R. Automated Ovarian Classification in Digital Ultrasound Images using SVM, International Journal of Engineering Research and Technology 2012; 1(6).

IntechOpen

IntechOpen